available at www.sciencedirect.com

ScienceDirect

journal homepage: www.elsevier.com/locate/jmbbm

Research paper

Effect of surface treatments on the fatigue life of titanium for biomedical applications

L. Pazos[a,*], *P. Corengia*[a,b], *H. Svoboda*[c]

[a] *Mechanics Research and Development Center, National Institute of Industrial Technology (INTI), Av. General Paz 5445, B1650WAB, San Martín, Buenos Aires, Argentina*

[b] *INASMET–Tecnalia, Mikeletegi 2, E-20009 Donostia-San Sebastián, Spain*

[c] *Laboratory of Materials and Structures, INTECIN, Faculty of Engineering, University of Buenos Aires, CONICET. Av. Las Heras 2214, C1427AAR, Buenos Aires, Argentina*

ARTICLE INFO

Article history:
Received 1 April 2009
Received in revised form
2 March 2010
Accepted 3 March 2010
Published online 16 March 2010

ABSTRACT

Many surface treatments that are used in cementless and endosseous implants modify the topography and the roughness to increase the implant-bone contact area and thus favor bio-mechanical anchorage, shortening the period of osseointegration. Nevertheless, the effects that the surface treatments can have on the fatigue life of the material are not generally considered. In this sense, the superficial condition of the component is one of the features that affect the fatigue strength, specially the fatigue crack nucleation.

The fatigue behaviour of annealed commercially pure titanium grade 4 was studied. The surface treatments used were acid etching, shot blasting and a dual treatment of blasting + acid etching. An as-machined surface condition was used as a reference. Topography, roughness, surface defects, microstructural changes and residual stresses were characterized in each case. Rotating-bending fatigue tests of each surface condition were conducted at room temperature with a frequency of 33 Hz. S–N curves and Basquin equations were obtained based on the results of these tests. Tested samples were also characterized to evaluate fatigue damage.

The acid etching decreases the fatigue endurance, while the blasting and blasting + acid etching treatments showed a similar behaviour with respect to the reference condition. For acid etching, the modifications introduced (stress raisers) contributed to accelerate the nucleation of cracks. On the other hand, the treatments with a blasting stage besides generating stress raisers, introduced compressive residual stresses and superficial plastic deformation that tend to improve the fatigue endurance of the material.

1. Introduction

Within the great family of biomaterials, metallic biomaterials are extensively utilized due to their wide range of applications in musculoskeletal implants, such as artificial hip and knee protheses; screws, plates, nails and intramedullar fixation devices; and dental implants (Hanawa, 1999). Titanium and its alloys are recognized within the biomaterials due to

* *Corresponding author.* Tel.: +54 11 4724 6297; fax: +54 11 4754 5986.
E-mail addresses: lpazos@inti.gob.ar (L. Pazos), pablo.corengia@inasmet.es (P. Corengia), hsvobod@fi.uba.ar (H. Svoboda).

1751-6161/$ - see front matter © 2010 Elsevier Ltd. All rights reserved.
doi:10.1016/j.jmbbm.2010.03.006

both their excellent biocompatibility and high chemical inertness of the oxide that covers their surfaces, as well as their mechanical and their osseointegration properties that promote their regular use in biomedical applications (Santana Guilherme et al., 2005; Cacciafesta et al., 2001; Long and Rack, 1998; Niinomi, 2008; Geetha et al., 2009; Liu et al., 2004).

In the case of titanium implants, surface roughness is one of the most important surface characteristic in reducing the period of osseointegration, stimulating greater bone regeneration and improving mechanical stability by interlocking the surrounding bone tissue with the implant (Göransson et al., 2003; Bagno and Di Bello, 2004; Lee et al., 2008). Indeed, the modifications introduced by surface treatments developed for cementless and endosseous implants are based on the empirical evidence that there is a surface roughness range where the osseointegration is optimized (Wennerberg et al., 1996a; Han et al., 1998; Lincks et al., 1998; Boyan et al., 1999; Deligianni et al., 2001).

Within the great variety of surface treatments used in biomaterials to improve osseointegration and to reduce the healing time, nowadays, blasting, acid etching and a combination of both (blasting + acid etching) are widely used (Le Guéhennec et al., 2007; Dimitriou and Babis, 2007).

The implants usually bear cyclic loads during their service life, and therefore, the fatigue endurance of the materials will play a very important role when trying to estimate the long-term performance of the device (Gil et al., 2007; Liu et al., 2004). Furthermore, the surface condition of an implant is one of the main features that can affect the fatigue properties, mainly the crack nucleation stage. The surface factors, which affect the fatigue life of a implant can be divided roughly into three categories: (i) surface roughness or stress raisers at the surface, (ii) changes in the fatigue strength of the surface metal, (iii) changes in the residual stress condition of the surface (Fernández Pariente and Guagliano, 2008; Webster and Ezeilo, 2001; Arola and Williams, 2002). Generally, the presence of notches in a loaded specimen accelerates the initial stage of crack growth (stage I), due to the stress raiser effect and the triaxiality produced at the root of the notch that lead to a high local stress and a decrease in the material yielding capacity. In contrast, the introduction of superficial compressive residual stresses (by means of blasting, thermomechanical treatments, etc.) can severely increase the fatigue strength. Therefore, although the surface treatments applied to bone engaging implants introduce important improvements in tissue responses, the fatigue life of the treated implants can be significantly affected, due to the residual stresses introduced during the treatment, the surface roughness, the generation of defects, the superficial hardening by plastic deformation, etc. (Jiang et al., 2006).

The aim of the present work is to study the effect of the surface treatments: blasting, acid etching and blasting + acid etching, in the fatigue life of commercially pure titanium. Additionally, the influence of the surface modifications introduced for each treatment is analyzed.

2. Materials and Methods

The experimental procedure was divided into three stages: (i) base material characterization, (ii) surface treatments' and surface characterization of treated samples, (iii) evaluation of the treatments effects on the fatigue life by rotating-bending fatigue tests and characterization of tested samples.

2.1. *Base material characterization*

The material studied was commercially pure (c.p.) titanium grade 4 in rods of 6.4 mm in diameter and flat samples of 18×18 mm^2 and 8 mm in thickness. Fatigue samples were machined from the rods.

The material characterization was carried out by metallographic analyses, tensile tests and Vickers microhardness measurements.

Metallographic samples were prepared to characterize the microstructure, which was etched with Kroll's reagent (10% HF, 5% HNO_3, 85% H_2O- Reagent No. 186 ASTM E407) (ASTM Standard E407, 2007). The mean grain size was determined according to the ASTM E112 (ASTM Standard E112, 2004). A Universal Machine Shimadzu UH-1000 kNA was employed for the tensile tests, where the ultimate tensile strength, yield strength, elongation and reduction in area were obtained. A Microhardness Tester Shimadzu HMV-2000 was used to obtain Vickers microhardness. The obtained results for the microhardness test were an average of five measurements.

2.2. *Execution of the surface treatments and their characterization*

Four different surface conditions were selected to evaluate their effects on the fatigue life: as-machined condition (M: without any surface treatment), acid etching (A), blasting (B), and dual treatment of blasting and acid etching (BA). The M condition was used as a reference.

A 9 M sulfuric acid solution at 60 °C was used in treatment A. Samples were soaked for 15 min. Treatment B was carried out using Al_2O_3 particles with a mean size within 425 and 600 μm. The process parameters were: 8 bar of working pressure, 60 to 80 mm of distance from the nozzle to the sample, approximately 90° of impact angle with respect to the sample surface. The BA treatment was carried out using the same conditions detailed above for A and B treatments. Treatment B was carried out in the first place followed by treatment A. These treatment conditions were used for both type of samples (fatigue and flat).

To characterize the different surface conditions, the following analyses were performed: (i) topography inspection, (ii) surface roughness measurement, (iii) surface defect and microstructure characterization, and (iv) residual stress analysis. (i), (ii) and (iii) were done on fatigue samples, while (iv) was done on flat samples.

2.2.1. *Topography*

Topography was characterized with a scanning electron microscope (SEM) Phillips model SEM 505. Besides, to confirm the presence of foreign particles embedded in the surfaces, energy dispersive spectroscopy (EDS) adapted to the SEM was performed.

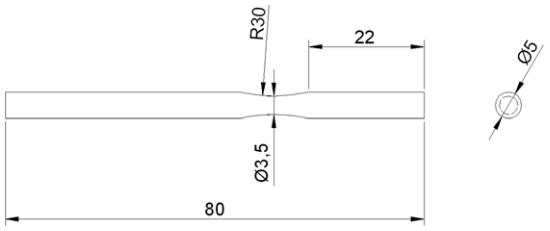

Fig. 1 – Geometry and dimensions of the fatigue samples (in millimeters).

2.2.2. *Roughness*

To characterize the superficial roughness, the mean roughness (R_a), total roughness (R_t) and the mean spacing (S_m) were determined using a Taylor Hobson model Surtronic 3 + profilometer. The values reported for each condition were the average of five measurements carried out on a fatigue sample. These measurements were done on five different generatrices of the sample.

2.2.3. *Surface defects and microstructure characterization*

Longitudinal sections of the fatigue samples were prepared for metallographic observation to investigate the surface and subsurface microstructure. Light microscopy (LM) and SEM were applied to characterize the superficial defects introduced and the changes produced on the material's microstructure.

2.2.4. *Residual stresses*

The presence of residual stresses was qualitatively analyzed with a RIGAKU diffractometer using radiation Cu-Kα (λ = 1.5418 Å) radiation by comparison between different treated samples. The X-ray pattern was obtained for the family of (2 1 3) planes, which diffracts at $2\theta = 139.5°$. A rough estimation of residual stress levels was carried out by means of expressions reported elsewhere (Webster and Ezeilo, 2001).

2.3. *Rotating-bending fatigue tests and characterization of tested samples*

The rotating-bending fatigue tests ($R = -1$) were conducted in a M.O.P. Type CT 8/30 machine at room temperature in air, with a frequency of 33.33 Hz (2000 rpm). The samples were tested with constant stress amplitude, at different load levels. The maximum stress applied was on the order of 2/3 of the ultimate tensile stress of the material. The number of cycles to failure was recorded at complete fracture of the specimens. A criterion of infinite life of 10^7 cycles was also adopted. The test configuration corresponds to a cantilever beam, loaded in an extreme. The geometry and dimensions of the samples can be observed in Fig. 1. The number of samples was $n = 5$ for the as-machined condition and at least $n = 10$ for the A, B, and BA surface treatments. σ_a–N_f curves were plotted based on the results of these tests. Tested samples were characterized by SEM and LM observations of longitudinal sections to evaluate the superficial damage.

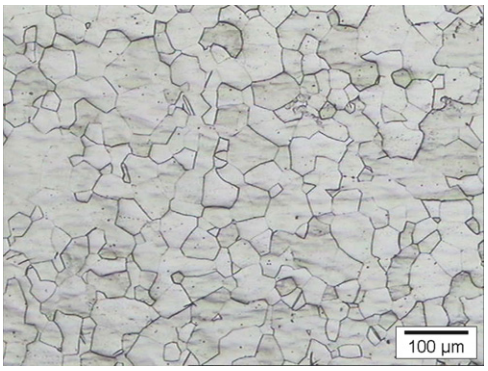

Fig. 2 – Microstructure of the starting material.

Table 1 – Tensile and microhardness test results.

σ_{UTS} (MPa)	$\sigma_{0.2}$ (MPa)	e (%)	A (%)	$HV_{(1N)}$
685	572	25.2	35.5	224 ± 10

3. Results

3.1. *Base material characterization*

Fig. 2 shows LM images of the microstructure of a cross section of the original material. The metallographic analysis revealed the presence of α phase equiaxial grains in both the longitudinal and cross section. The mean grain size measured was No. 7 according to the ASTM E112 using the comparative method A (Sheet II) (ASTM Standard E112, 2004). The values obtained from the tensile and microhardness tests are gathered in Table 1. These data meet the requirements of the ASTM F67 standard for commercially pure titanium grade 4 (ASTM Standard F67, 2006).

3.2. *Surface treatment characterization*

3.2.1. *Topography*

The analysis of the surfaces by SEM indicated that the topographies obtained were similar to those reported in the literature (Li et al., 2002; Ban et al., 2006; Cho and Park, 2003; Pegueroles et al., 2008; Aparicio et al., 2002; Wennerberg et al., 1996b). Fig. 3 shows SEM images of the different surfaces studied. Fig. 3(a), corresponding to the M condition, reveals equidistant parallel marks characteristics of the machining process. Treatment A introduced modifications in the sample topography, as shown in Fig. 3(b). Microholes characteristic of this treatment are clearly observed (Li et al., 2002). In some cases, intergranular corrosion could be detected. This feature has been reported as a topographical characteristic of acid etched surfaces in osseointegration studies (Ban et al., 2006; Cho and Park, 2003). The B-samples presented an irregular rough surface with evidence of plastic deformation and material tearing (Fig. 3(c)), and embedded particles were occasionally found. These irregularities presented a random distribution, which was also reported by other authors (Pegueroles et al., 2008; Aparicio et al., 2002; Wennerberg et al., 1996b). Regarding the topography produced by BA

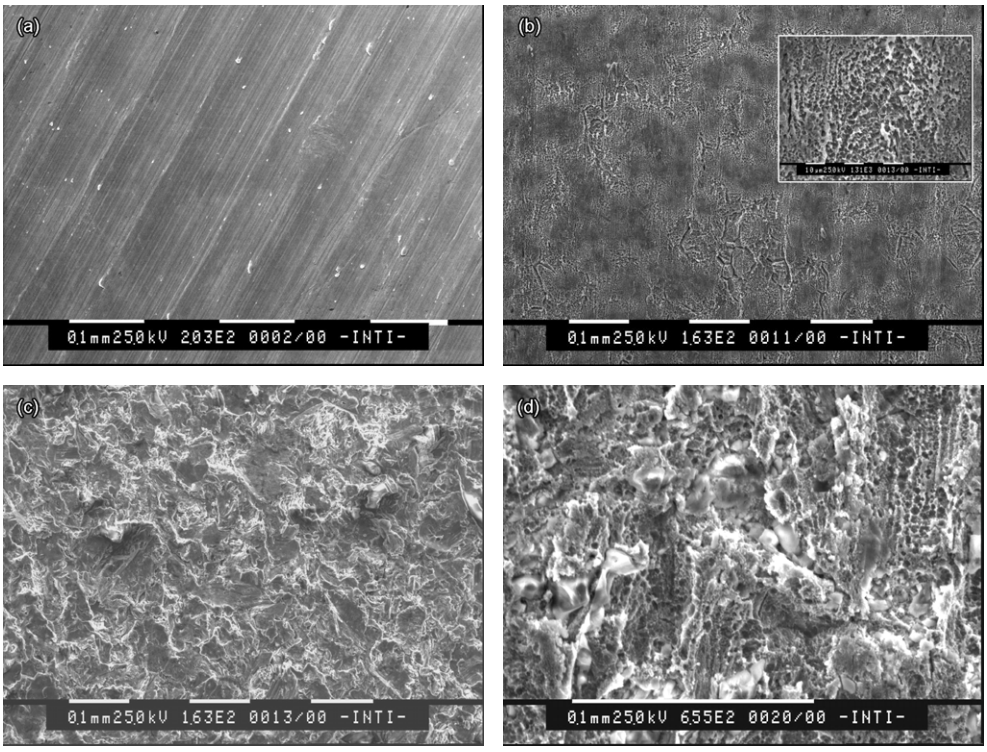

Fig. 3 – SEM images of the different sample surfaces (a) M-surface (200×); (b) A-surface (160×); (c) B-surface (160×); (d) BA-surface (650×).

treatment, Fig. 3(d) evidences a rough surface with a two-level roughness in agreement with the literature (Li et al., 2002; Conforto et al., 2004). At low magnifications, the SEM images revealed irregularities which were similar to the ones observed in B-samples, while at higher magnification, the microholes characteristic of treatment A could be observed. The distribution of the microholes was homogeneous in the whole surface and zones with severe attack but corroded grain boundaries as in the A-samples were not differentiated.

3.2.2. *Roughness*

The results of the surface roughness measurements are reported in Table 2 for each condition. The values of R_a, R_t and S_m obtained are expressed with their standard deviation (D). All the treatments increased the roughness parameters with respect to the *M* condition. For the R_a, this increase was about 3 μm. The values obtained in the present work are similar to those reported in the literature for these types of treatments and they are within the roughness range that improves osseointegration (Le Guéhennec et al., 2007; Gil et al., 2007; Aparicio et al., 2002; Cooper, 2000). The A treatment presented the lowest R_a value, while the B and BA treatments produced similar R_a values. The results of the R_t measurements show a similar tendency to that obtained for the R_a values. In contrast, the treatment that showed greater S_m was A, while the BA treatment caused the smallest S_m value.

3.2.3. *Surface defects and microstructure characterization*

The material microstructure near the surface for each studied condition is shown in Fig. 4. No severe superficial defects were observed in the M-sample (Fig. 4(a)). Treatment A did not modify substantially the macroscopic profile of the surface with respect to the reference condition as can be appreciated in Fig. 4(b). However, at higher magnifications the profile associated with the microholes and the intergranular corrosion previously mentioned, was observed. Here, V-shaped notches could be distinguished at the grain boundaries.

Table 2 – Roughness parameters measured.

Type of surface	$R_a \pm D$ (μm)	$R_t \pm D$ (μm)	$S_m \pm D$ (μm)
M	0.79 ± 0.10	5.95 ± 0.61	59.25 ± 10.44
A	3.30 ± 0.63	24.0 ± 3.78	102.9 ± 20.01
B	4.28 ± 0.78	32.2 ± 4.42	95.8 ± 12.17
BA	4.42 ± 0.37	35.0 ± 5.55	89.8 ± 9.36

Fig. 4(c) shows the severely plastically deformed surface layer produced in the B-samples. The deformed layer was relatively uniform along the entire treated surface with a thickness ranging from 10 to 20 μm. Twinning was the predominant deformation mode in the region below the severely deformed surface layer, as expected for this type of material (Jiang et al., 2006). In addition, notch-shaped superficial defects were distinguished. They were associated with the sharp edges of the alumina particles. The dimensions of these defects were greater than the ones observed on the A-samples. A detail of a particle embedded on the surface and its EDS pattern are shown in Fig. 5. The spectrum observed in Fig. 5(b) reveals a significant Al content in the particle, which

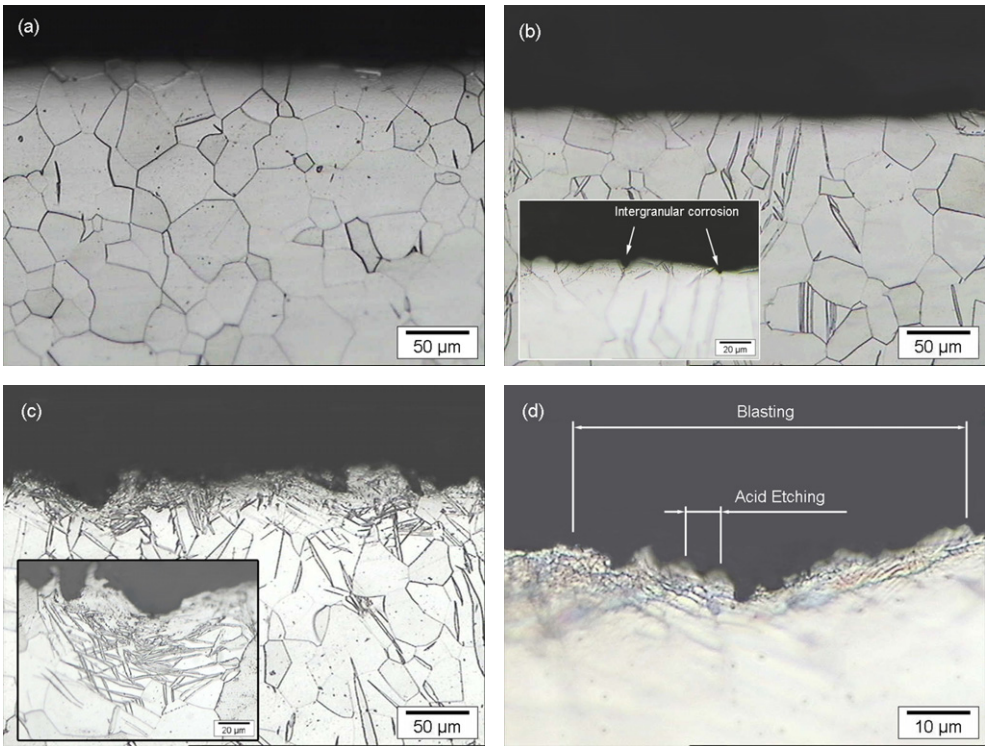

Fig. 4 – LM images of longitudinal sections of the samples (a) M (200×); (b) A (200× and 500×); (c) B (200× and 500×); (d) BA (1000×).

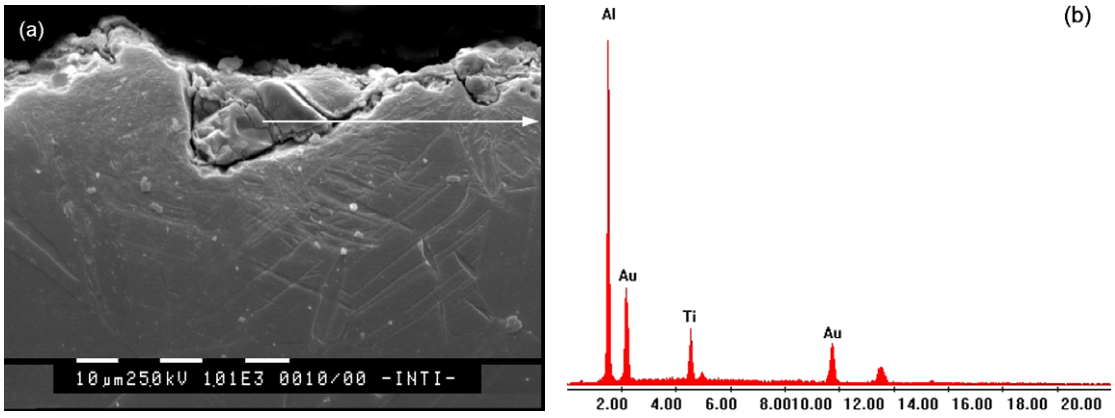

Fig. 5 – (a) SEM image of a longitudinal section of a fatigue sample with a particle of Al_2O_3 embedded, (b) EDS pattern of the particle.

indicates that it is one of the alumina particles employed in treatment B. The presence of gold in the spectrum is associated with the sputter coating used for the sample preparation.

The surface profile generated by the BA treatment observed at low magnification was similar to the profile of the B-surface. A severely deformed surface layer and notch-shaped defects were also observed over the whole treated surface. Nevertheless, at higher magnifications microholes produced by treatment A could be distinguished as well (Fig. 4(d)). Furthermore, the distribution of these microholes was homogeneous in the whole surface, with neither zones with differentiated etching nor significant intergranular corrosion being detected.

3.2.4. *Residual stresses*

Fig. 6 shows the Intensity vs. 2θ graph obtained around the angle $2\theta = 139.5°$ for every analyzed condition. The estimated residual stresses were around zero for the M and A condition. Nevertheless, the M condition presented slightly tensile stresses as could be expected for this type of process (Sasahara, 2005). The peaks corresponding to treatments involving the blasting stage (B and BA treatments) appeared shifted towards lower angles and were also wider than for the other conditions. These results were associated with the existence of compressive residual stresses (Cullity and Stock, 2001) and were estimated in the range of 280–380 MPa. This result is in agreement with those expected for blasted titanium (Jiang et al., 2006). Furthermore, a decrease of the

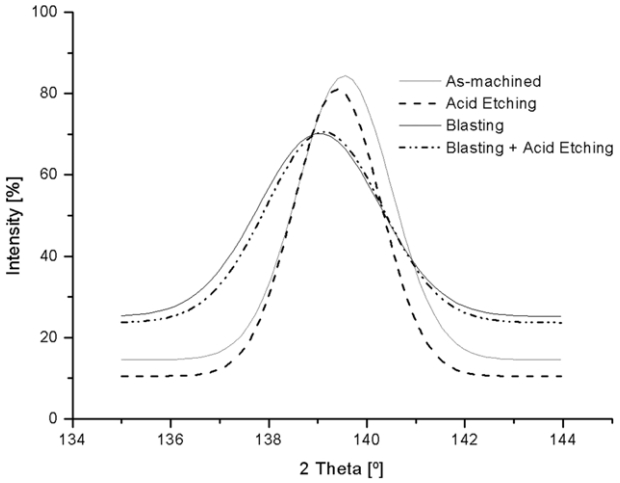

Fig. 6 – XRD pattern obtained for the M-, A-, B- and BA-surfaces.

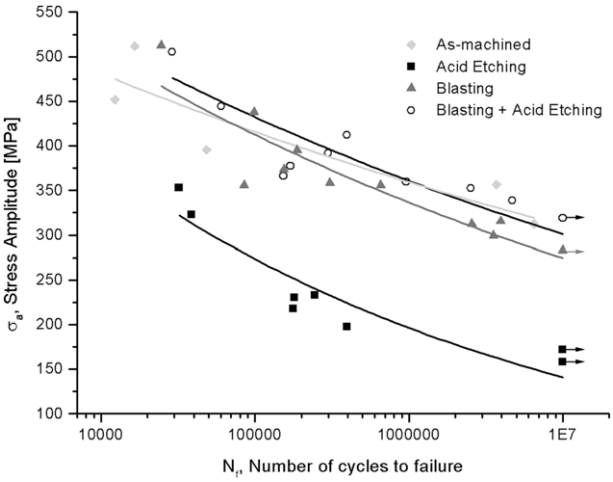

Fig. 7 – σ_a–N_f curves.

intensity was observed for these peaks, which implies the occurrence of a certain texture in the treated surfaces (Cullity and Stock, 2001).

3.3. *Rotating-bending fatigue test and characterization of tested samples*

3.3.1. *Rotating-bending fatigue test*

Fig. 7 shows the measured σ_a–N_f curves for every surface condition. Experimental data were fitted with the Basquin equation, which is used for modelling this type of tests. The values obtained for the M condition are consistent with data previously reported (Lin et al., 2005). For the A condition the fatigue strength was approximately 150 MPa smaller than for the M-samples in the whole analyzed range. In terms of fatigue life, for a given stress amplitude, the decrease of the number of cycles to failure was around 2 orders of magnitude. On the other hand, the B-, BA- and M-samples showed similar results. Nevertheless, the fatigue life obtained for the BA condition tended to be slightly over that of the B condition. All the values obtained are within the usual scatter for this type of tests (Long and Rack, 1998; Lin et al., 2005). The Basquin equation's constants and the correlation factors R^2 obtained from every fitting are:

$$M: \sigma_a = 811.9 * N_f^{-0.058} \qquad R^2 = 0.8290$$
$$A: \sigma_a = 1016.3 * N_f^{-0.121} \qquad R^2 = 0.7945$$
$$B: \sigma_a = 1060.8 * N_f^{-0.083} \qquad R^2 = 0.8435$$
$$BA: \sigma_a = 878.2 * N_f^{-0.063} \qquad R^2 = 0.7864$$

These expressions provide useful information for design, because they allow modelling of the material fatigue behavior for each surface treatment.

3.3.2. *Superficial damage*

Fig. 8 shows images of longitudinal sections of the tested samples. As can be seen, the superficial defects acted as stress raisers and were preferential sites for fatigue crack nucleation. The sample with treatment A showed a larger amount of fatigue cracks, which were longer than those observed for the other surface treatments. In the case of B, BA and M conditions, few cracks were detected, even in samples tested at high stress amplitudes. In the M condition, the cracks nucleated from a smooth surface without severe superficial defects. The nucleation mechanisms involved were related to strain concentration and cyclic sliding (Xiaoli and Haicheng, 1996; Ismarrubiea and Suganob, 2004). Moreover, deformation twins and secondary cracks were observed (Fig. 8(a)). Nucleation of fatigue cracks was observed at the V-shaped superficial defects of the A-samples, which acted as stress raisers (Fig. 8(b)). As shown in Fig. 8(c), the notches originated by the alumina particles projection, acted as stress raisers and were preferential sites for the fatigue crack nucleation in the B-samples. In BA-specimens the fatigue crack nucleation also took place at notches generated during treatment B (Fig. 8(d)). Nevertheless, fatigue cracks were not nucleated at the surface defects caused by treatment A after treatment B. Therefore, it is concluded that the microholes generated by treatment A were not preferential sites for fatigue crack nucleation in a BA-surface.

4. Discussion

4.1. *General considerations on the surface treatment effects*

It is known that fatigue life, related to fatigue crack nucleation, could be affected by several factors like roughness, surface defects –acting as stress raisers–, surface hardening and residual stresses, among others (Jiang et al., 2006; Wagner, 1999). Table 3 summarizes the effects produced by each treatment with the aim of carrying out a qualitative analysis of the relative importance regarding fatigue life of the different surface modifications.

The defects produced by treatment A resulted from a generalized surface corrosion (microholes + intergranular corrosion). Intergranular corrosion defects were more severe stress raisers than microholes, promoting crack nucleation due to their geometry and location.

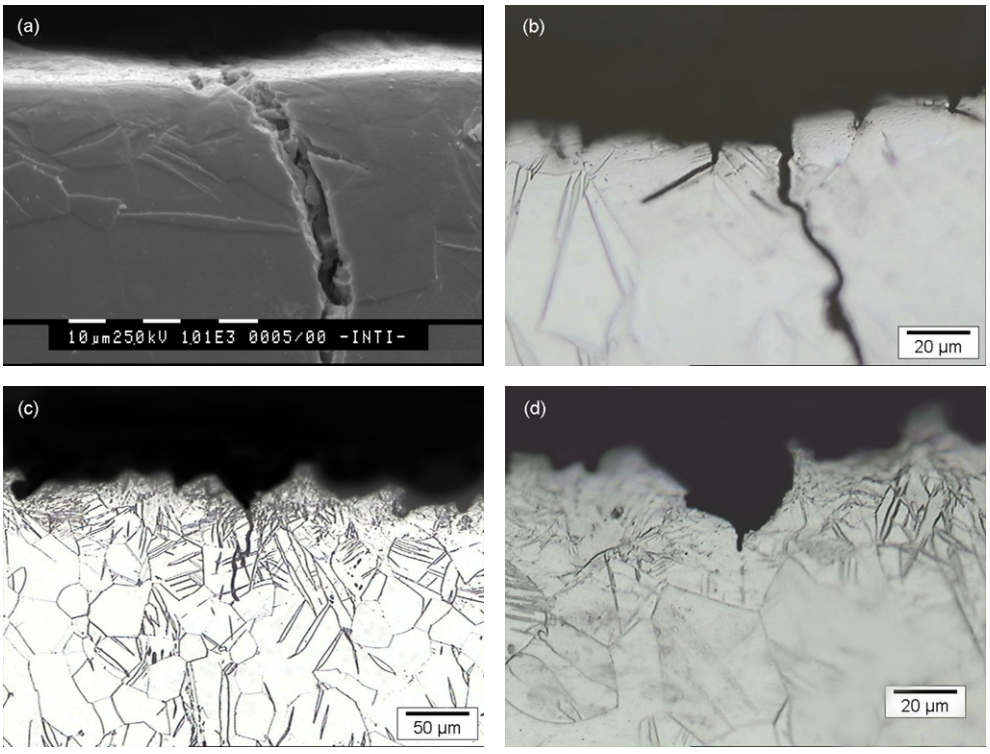

Fig. 8 – LM and SEM images of fatigue crack nucleated. (a) M-sample (1000×); (b) A-sample (500×); (c) B-sample (200×); (d) BA-sample (500×).

Table 3 – Summary of modifications introduced by the surface treatments.

Type of surface	Roughness	Superficial defects	Superficial plastic deformation	Residual stresses	Fatigue life
M	Reference surface	Reference surface	Reference surface	Reference surface	Reference values
A	Increase roughness	Generate stress raisers	Not produce superficial plastic deformation	Not introduce residual stresses	Decrease by about 150 MPa
B	Increase roughness	Generate stress raisers	Produce superficial plastic deformation	Introduce residual stresses	Similar to reference values
BA	Increase roughness	Generate stress raisers	Produce superficial plastic deformation	Introduce residual stresses	Similar to reference values

The surface defects generated in samples with a blasting stage (B- and BA-) were randomly distributed on the studied surface samples. The obtained results showed that the geometry of these defects is closely related to the alumina particle geometry. The notches were associated to the sharp edges of the particles, which was confirmed by the observation of alumina particles embedded in the surface. It is interesting to establish the differences in the effect of treatment A on the material surface, depending on the presence or not of the prior treatment B. As mentioned previously, treatment A produces microholes and intergranular attack. For the case of treatment A after B no evidence of intergranular attack was observed. This would be explained due to the plastic deformation introduced during the B treatment that increases the surface energy, diminishing considerably the greater grain boundary activity. Thus, treatment A after B, finds a homogeneous surface without a definite grain boundary feasible to be attacked, and produces a superficial modification with homogeneously distributed microholes.

In comparison with the M condition, the surface treatments significantly increased the surface roughness of the samples along with the generation of superficial defects. Although the generation of surface defects led to a roughness increase, the observations of the surface profiles showed that the defects had geometric features and distributions that the contact profilometry did not differentiate. Therefore, although the roughness measurement is an important technique to characterize surfaces for biomedical applications, in this case, the roughness values obtained by a contact profilometer are not the most suitable features to explain the effects of the different surface treatments in fatigue life, because they do not differentiate between the characteristics of the defects generated by them. In this work, the roughness values measured on the treated surfaces had no major differences, but in term of stress concentration, the stress raisers

generated by treatment A were more severe than the ones generated by the B or BA treatments. Alternative methods such as light interferometry should be used to avoid this problem (Ås et al., 2005, 2008).

The A treatment did not generate either superficial plastic deformation or residual stresses. The treatments involving blasting can introduce compressive residual stresses and strain hardening at the surface, thus the material fatigue endurance can be sensitively affected (Jiang et al., 2006; Kobayashi et al., 1998). As evidenced in the XRD patterns (Fig. 6), the B and BA treatments introduced compressive residual stresses. In addition, the appearance of a severely deformed surface layer with a twinning zone in the subsurface, evidence a strain hardening by cold working (Jiang et al., 2006).

4.2. *Fatigue life*

The A-samples presented a worse fatigue performance than the other analyzed conditions. As mentioned previously, this treatment introduced neither superficial plastic deformation nor induced considerable residual stresses with respect to the reference condition. Nevertheless, the treatment generated defects that acted as effective stress raisers for fatigue crack nucleation. In this sense, the decrease in fatigue life of the A-samples would be linked to the decrease of the number of cycles that are necessary for the nucleation of fatigue cracks from the preexisting defects. This is consistent with the larger amount of propagating cracks of greater length observed in the A-samples (Fig. 8(b)). Treatments introducing compressive residual stresses had a better fatigue performance than the A treatment. This result is in agreement with the bibliography since the compressive residual stresses can reduce and even eliminate the effects of the stress raisers (Jiang et al., 2006). Furthermore, the severe plastic deformation gave rise to strain hardening in the surface layer that improve the fatigue behavior. Therefore, the B and BA conditions are more favorable.

5. Conclusions

A metallurgic-mechanical analysis has been applied to explain the effect of surface treatments on the fatigue life of c.p. titanium. Surface treatments use to improve osseointegration properties of metallic implants were characterized. The different surface modifications produced by the blasting, acid etching and blasting + etching treatments have been characterized according to the location and geometry of surface defects, surface hardening, and compressive residual stresses. A strong dependence of the fatigue crack nucleation mechanism on the surface conditions was observed. Acid etching treatment generated stress raisers, but neither introduced compressive residual stresses nor hardened the surface, and was the treatment that showed a lower fatigue endurance of titanium. On the other hand, treatments with a blasting stage had a better fatigue behavior that was associated to the presence of a severely plastic deformed surface layer, the strain-hardening related to it, and the compressive residual stresses. This fact counteracts the negative effect in fatigue life of the stress raisers introduced by the treatments.

Acknowledgements

The authors are very grateful to RosterDent S.A. for kindly donating the material and the blasting treatments. The XRD support of the Laboratory of Amorphous Solids, FIUBA, is gratefully acknowledged. The authors want to thank the collaboration received from the staff of the Laboratory of Materials and Structures, FIUBA, and the Center of Mechanic Research and Development, INTI, for their technical support.

REFERENCES

Aparicio, C., et al., 2002. Human-osteoblast proliferation and differentiation on grit-blasted and bioactive titanium for dental applications. Journal of Materials Science 13, 1105–1111.

Arola, D., Williams, C.L., 2002. Estimating the fatigue stress concentration factor of machined surfaces. International Journal of Fatigue 24, 923–930.

Ås, S.K., et al., 2005. Fatigue life prediction of machined components using finite element analysis of surface topography. International Journal of Fatigue 27, 1590–1596.

Ås, S.K., et al., 2008. Surface roughness characterization for fatigue life predictions using finite element analysis. International Journal of Fatigue 30, 2200–2209.

ASTM Standard E112, 2004. Standard test methods for determining average grain size. ASTM International, West Conshohocken, PA, doi:10.1520/E0112-96R04E02, www.astm.org.

ASTM Standard E407, 2007. Standard practice for microetching metals and alloys. ASTM International, West Conshohocken, PA, doi:10.1520/E0407-07, www.astm.org.

ASTM Standard F67, 2006. Standard specification for unalloyed titanium, for surgical implant applications (UNS R50250, UNS R50400, UNS R50550, UNS R50700). ASTM International, West Conshohocken, PA, doi:10.1520/F0067-06, www.astm.org.

Bagno, A., Di Bello, C., 2004. Surface treatments and roughness properties of Ti-based biomaterials. Journal of Materials Science — Materials in Medicine 15, 935–949.

Ban, S., et al., 2006. Surface modification of titanium by etching in concentrated sulfuric acid. Dental Materials 22, 1115–1120.

Boyan, B.D., et al., 1999. Surface roughness mediates its effects on osteoblasts via protein kinase A and phospholipase A2. Biomaterials 20, 2305–2310.

Cacciafesta, P., et al., 2001. Visualisation of human plasma fibrinogen adsorbed on titanium implant surfaces with different roughness. Surface Science 491, 405–420.

Cho, S.A., Park, K.T., 2003. The removal torque of titanium screw inserted in rabbit tibia treated by dual acid etching. Biomaterials 24, 3611–3617.

Conforto, E., et al., 2004. Rough surfaces of titanium and titanium alloys for implants and prostheses. Materials Science and Engineering C24, 611–618.

Cooper, L., 2000. A role for surface topography in creating and maintaining bone at titanium endosseous implants. Journal of Prosthetic Dentistry 84, 522–534.

Cullity, B.D., Stock, S.R., 2001. Elements of X-Ray Diffraction, third edition. Prentice Hall, New Jersey.

Deligianni, D.D., et al., 2001. Effect of surface roughness of the titanium alloy Ti–6Al–4V on human bone marrow cell response and on protein absorption. Biomaterials 22, 1241–1251.

Dimitriou, R., Babis, G.C., 2007. Biomaterial osseointegration. Enhancement with biophysical stimulation. Journal of Musculoskelet Neuronal Interact 7 (3), 253–265.

Fernández Pariente, I., Guagliano, M., 2008. About the role of residual stresses and surface work hardening on fatigue ΔKth of a nitrided and shot peened low-alloy steel. Surface & Coatings Technology 202, 3072–3080.

Geetha, M., et al., 2009. Ti based biomaterials, the ultimate choice for orthopaedic implants — a review. Progress Materials Science 54, 397–425.

Gil, F.J., et al., 2007. The effect of shot blasting and heat treatment on the fatigue behavior of titanium for dental implant applications. Dental Materials 23, 486–491.

Göransson, A., et al., 2003. Bone formation after 4 weeks around blood-plasma-modified titanium implants with varying surface topographies: an in vivo study. Biomaterials 24, 197–205.

Han, C., et al., 1998. Quantitative and qualitative investigation of surface enlarged titanium and titanium alloy implants. Clinical Oral Implants Research 9, 1–10.

Hanawa, T., 1999. In vivo metallic biomaterials and surface modification. Materials Science and Engineering A267, 260–266.

Ismarrubiea, Z.N., Suganob, M., 2004. Environmental effects on fatigue failure micromechanisms in titanium. Materials Science and Engineering A386, 222–233.

Jiang, X.P., et al., 2006. Enhancement of fatigue and corrosion properties of pure Ti by sandblasting. Materials Science and Engineering A429, 30–35.

Kobayashi, M., et al., 1998. Mechanism of creation of compressive residual stress by shot peening. International Journal of Fatigue 20, 351–357.

Le Guéhennec, L., et al., 2007. Surface treatments of titanium dental implants for rapid osseointegration. Dental Materials 23, 844–854.

Lee, B.H., et al., 2008. Effect of surface structure on biomechanical properties and osseointegration. Materials Science and Engineering C28, 1448–1461.

Li, D., et al., 2002. Biomechanical comparison of the sandblasted and acid-etched and the machined and acid-etched titanium surface for dental implants. Journal of Biomedical Materials Research 60, 325–332.

Lin, C., et al., 2005. A comparison of the fatigue behavior of cast Ti–7.5Mo with c.p. titanium, Ti–6Al–4V and Ti–13Nb–13Zr alloys. Biomaterials 26, 2899–2907.

Lincks, J., et al., 1998. Response of MG63 osteoblast-like cells to titanium and titanium alloy is dependent on surface roughness and composition. Biomaterials 19, 2219–2232.

Liu, X., et al., 2004. Surface modification of titanium, titanium alloys, and related materials for biomedical applications. Materials Science and Engineering R47, 49–121.

Long, M., Rack, H.J., 1998. Titanium alloy in total joint replacement: a material science perspective. Biomaterials 19, 1621–1639.

Niinomi, M., 2008. Mechanical biocompatibilities of titanium alloys for biomedical applications. Journal of the Mechanical Behavior of Biomedical Materials 1, 30–42.

Pegueroles, M., et al., 2008. The influence of blasting and sterilization on static and time-related wettability and surface-energy properties of titanium surfaces. Surface & Coatings Technology 202, 3470–3479.

Santana Guilherme, A., et al., 2005. Surface roughness and fatigue performance of commercially pure titanium and Ti-6Al-4V alloy after different polishing protocols. Journal of Prosthetic Dentistry 93, 378–385.

Sasahara, H., 2005. The effect on fatigue life of residual stress and surface hardness resulting from different cutting conditions of 0.45%C steel. International Journal of Machine Tools & Manufacture 45, 131–136.

Wagner, L., 1999. Mechanical surface treatments on titanium, aluminum and magnesium alloys. Materials Science and Engineering A263, 210–216.

Webster, G.A., Ezeilo, A.N., 2001. Residual stress distributions and their influence on fatigue lifetimes. International Journal of Fatigue 23, S375–S383.

Wennerberg, A., et al., 1996a. Bone tissue response to commercially pure titanium implants blasted with fine and coarse particles of aluminium oxide. International Journal of Oral & Maxillofacial Implants 11, 38–45.

Wennerberg, A., et al., 1996b. Torque and histomorphometric evaluation of c.p. titanium screws blasted with 25- and 75-μm-sized particles of Al_2O_3. Journal of Biomedical Materials Research 30, 251–260.

Xiaoli, T., Haicheng, G., 1996. Fatigue crack initiation in high-purity titanium crystals. International Journal of Fatigue 18, 329–333.